



A Journal of the Gesellschaft Deutscher Chemiker

Angewandte Chemie

GDCh

International Edition

www.angewandte.org

Accepted Article

Title: Phototriggered release of transmembrane chloride carrier from an o-nitrobenzyl-linked procarrier

Authors: Swati Bansi Salunke, Javid Ahmad Malla, and Pinaki Talukdar

This manuscript has been accepted after peer review and appears as an Accepted Article online prior to editing, proofing, and formal publication of the final Version of Record (VoR). This work is currently citable by using the Digital Object Identifier (DOI) given below. The VoR will be published online in Early View as soon as possible and may be different to this Accepted Article as a result of editing. Readers should obtain the VoR from the journal website shown below when it is published to ensure accuracy of information. The authors are responsible for the content of this Accepted Article.

To be cited as: *Angew. Chem. Int. Ed.* 10.1002/anie.201900869
Angew. Chem. 10.1002/ange.201900869

Link to VoR: <http://dx.doi.org/10.1002/anie.201900869>
<http://dx.doi.org/10.1002/ange.201900869>

Phototriggered release of transmembrane chloride carrier from an *o*-nitrobenzyl-linked procarrier

Swati Bansi Salunke,^[a] Javid Ahmad Malla,^[a] and Pinaki Talukdar*^[a]

Abstract: While there have been tremendous studies about synthetic chloride carriers and their recent application in the apoptotic cell death, so far the proposed huge potential of these systems in targeting cancer has not been materialized due to their cytotoxicity to healthy cells as well. Herein, we describe the development of an indole-2-carboxamide receptor as an efficient membrane chloride carrier while the corresponding *o*-nitrobenzyl-linked derivative is a procarrier of the ion. Photoirradiation of the procarrier in liposomes results in the release of the active carrier displaying up to 90% transport efficiency. Such photorelease of the carrier also works within cancer cells resulting in efficient cell death. All in all, such photocleavable procarriers have great potential as a photodynamic therapy to combat various types of cancers.

In classical anticancer chemotherapy, the drugs target specific genes or proteins/enzymes found in cancer cells to trigger apoptosis induction and related cell death networks to eliminate malignant cells.^[1] However, the activation of different anti-apoptotic pathways,^[2] mutations in the drug targets that prevent the binding of the drug,^[3] and over-expression of proteins that compensate for the loss of the drug target^[4] are known to cause tumor survival, therapeutic resistance, and recurrence of cancer. The cellular apoptosis is also linked to the homeostasis of several ions e.g., sodium, potassium, calcium, and chloride.^[5] In literature, several biomimetic synthetic systems have been reported for transporting ions across the lipid membrane.^[6] Recently, natural and synthetic chloride transporters, e.g., prodigiosin,^[7] tambjamine,^[8] ureas/thioureas,^[9] calix[4]pyrroles,^[10] squaramides,^[11] and bis-sulfonamides^[12] causing apoptosis-mediated cancer cell death were also reported. These molecules function in the lipid membrane, unlike binding to any specific genes or proteins/enzymes, and perturb the intracellular chloride ion concentration to kill the cells. Therefore, in principle, synthetic chloride transporters can overcome the resistance related to the mutations and over-expression of genes and proteins. However, chloride transport-mediated death was also observed for normal cells as an undesired consequence. This toxicity is considered as a limitation for applying ion transporters in anticancer therapy. Therefore, there is a need to develop stimuli-responsive systems, which can be applied selectively for cancer cells. In this line, pH was used primarily to activate the ion transports in specific pH-ranges.^[13] Recently, enzymes (esterase and glycosylase) were

used for releasing active ion carrier from a procarrier (i.e. the inactive form of the carrier molecule).^[14] Photoisomerization of molecules, on the other hand, was used to activate or deactivate channel/carrier mediated ion transport.^[15]

Herein, we have introduced the “photocleavable prodrug” concept in the domain of artificial ion transporters and developed a procarrier that endows photo-controlled release of an active carrier to induce chloride mediated cell death. Photocleavable protecting groups are well-known in organic synthesis for several decades,^[16] and recently have had a rejuvenation in recent years due to their extensive application in biology.^[17] For example, phototriggered removal of the *o*-nitrobenzyl (ONB) group^[18] was successfully applied for either delivery^[19] or activation^[20] of anticancer drugs. Mo et. al. have illustrated the photoactivation of an anticancer prodrug to release the 5-fluorouracil (an anticancer drug to treat solid cancers, such as colon, breast, rectal, and pancreatic cancers), and induce cellular apoptosis.^[20d] Photocleavable prodrugs have already shown promises in the photodynamic anticancer therapy. Such remarkable literature support provoked us designing an ONB-linked *N*-aryl-1*H*-indole-2-carboxamide procarrier (Figure 1A).

In this design, the *N*-phenyl-1*H*-indole-2-carboxamides **1a-1d** were selected as carrier molecules (Figure 1B). The *para*-substituent of the phenyl ring was changed among R = -CH₃, -C(CH₃)₃, -Br and -CF₃ to vary the acidity of N-H_b proton (Table S1). Theoretical estimation based on the calculator plugins of MarvinSketch program^[21] gave p*K*_a = 14.31, 14.23, 13.89 and 13.86 for the N-H_b protons of **1a-1d**, respectively, suggesting the higher acidity of the proton when a stronger electron withdrawing R group was used. The R groups also influenced the acidity of N-H_a protons in the same way (i.e., p*K*_a = 11.85, 11.85, 11.77 and 11.76 for **1a-1d**, respectively). The program

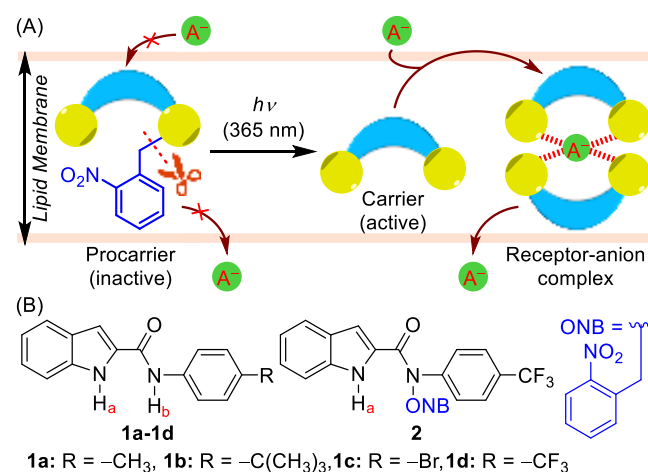


Figure 1. Phototriggered release of an anion carrier from corresponding ONB protected procarrier (A). Structures of carriers **1a-1d** and a procarrier **2** (B).

[a] S B Salunke, J A Malla, Dr. P Talukdar
Chemistry Department
Indian Institute of Science Education and Research Pune
Dr. Homi Bhabha Road, Pashan, Pune 411008, Maharashtra (India)
E-mail: ptalukdar@iiserpune.ac.in

Supporting information for this article is given via a link at the end of the document.

was further useful in predicting the membrane permeability of these molecules, $\log P = 3.60, 4.63, 3.85$ and 3.96 for **1a-1d**, respectively. Molecule **2** was designed as the procarrier form of **1d**. Relatively higher $pK_a = 11.85$ for N-H_a proton and the absence of the N-H_b proton were considered as crucial limitations of **2** to be an anion transporter although, its amphiphilicity (i.e., $\log P = 5.49$) was ideal for the membrane permeation. Compounds **1a-1d** were synthesized by the coupling of indole-2-carboxylic acid **3** with *para*-substituted aniline derivatives **4a-4d** in the presence of EDC·HCl and HOBt (Scheme S1). Prior to the synthesis of **2**, compound **5** was prepared by the reductive amination of *o*-nitrobenzaldehyde and **4d** (Scheme S2). Subsequently, compound **3** was treated with SOCl₂ followed by the reaction with **5** in the presence of DMAP to get **2** in 92% yield (Scheme S3).

At first, the Cl⁻ ion binding properties of **1a-1d** were verified by ¹H NMR titration experiments in CD₃CN. Upon addition of tetrabutylammonium chloride (TBACl) to **1a-1d** (5 mM), downfield shifts of H_a, H_b, and H_c protons were observed indicating the interactions of these protons with the Cl⁻ ion (Figure S1–S4). The Job's plot analysis based on the change in N-H_a proton chemical shift of **1a-1d** confirmed the 1:1 complexation of the receptor and Cl⁻ (Figure S7). The binding constant, $K_a = 599.43 \pm 12.57 \text{ M}^{-1}$ was also calculated for **1d** using Bindfit program (Figure S4).^[22] Cl⁻ ion binding constants for **1a** ($K_a = 281.76 \pm 3.47 \text{ M}^{-1}$), **1b** ($K_a = 505.73 \pm 15.1 \text{ M}^{-1}$), and **1c** ($K_a = 656.14 \pm 9.20 \text{ M}^{-1}$) were relatively poor (Figure S1–S3). The ¹H NMR titration of **1d** with Br⁻ showed 1:1 and 1:2 binding stoichiometries with $K_{a(1:1)} = 103.31 \pm 2.45 \text{ M}^{-1}$ and $K_{a(1:2)} = 9.83 \pm 1.04 \text{ M}^{-1}$, respectively (Figure S5). The binding constant of **1d** with I⁻ could not be calculated precisely due to the insufficient shifts of the H_a, H_b, and H_c protons (Figure S6).

The ion transport properties of compounds **1a-1d** and **2** were examined across large unilamellar vesicles (LUVs), which were prepared from egg-yolk phosphatidylcholine (EYPC) lipids by entrapping 8-hydroxypyrene-1,3,6-trisulfonate (HPTS, 1 mM) dye in the buffer containing 1 mM HPTS, 10 mM HEPES and 100 mM NaCl (see ESI).^[12] The collapse of the applied pH gradient ($\text{pH}_{\text{in}} = 7.0$ and, $\text{pH}_{\text{out}} = 7.8$) upon addition of each compound was monitored by measuring the change in HPTS fluorescence at $\lambda_{\text{em}} = 510 \text{ nm}$ ($\lambda_{\text{ex}} = 450 \text{ nm}$) with time. The comparative ion transport activity of **1a-1d** at concentration $c = 400 \text{ nM}$ provided ion transport activity sequence: **1d** >> **1c** > **1b** ~ **1a** which suggests the roles of N-H proton acidity as well as $\log P$ values in the transport activity (Figure 2A). Compound **2** was inactive at this concentration, suggesting that it is a procarrier of ion as its ONB group acts as a barrier for efficient ion binding. The concentration profile of **1d** provided the effective concentration at 50% activity, $EC_{50} = 0.219 \mu\text{M}$ (i.e., compound/lipid ratio = 0.327 mol%). The Hill coefficient, $n = 1.88$ indicates the involvement of two molecules of **1d** in the active transporter formation (Figure S9). For **1c**, the EC_{50} and n values were $0.768 \mu\text{M}$ and 2.72 , respectively (Figure S10). EC_{50} and n values of **1a** and **1b** could not be determined due to the precipitation of these compounds at high concentrations.

The most active *N*-aryl-1*H*-indole-2-carboxamide **1d** was then studied for its ion selectivity across EYPC–LUVs⇌HPTS.

Variation of external cations (i.e., $\text{M}^+ = \text{Li}^+, \text{Na}^+, \text{K}^+, \text{Rb}^+$, and Cs^+) in the aforementioned LUVs did not provide any noticeable difference in the ion transport rate indicating no role of alkali metal cations in the transport process (Figure S12). However, the change of external anions (i.e., $\text{X} = \text{F}^-, \text{Cl}^-, \text{Br}^-, \text{OAc}^-$, and NO_3^-) in the EYPC–LUVs⇌HPTS provided a significant variation of ion transport activity (Figure 2B). To determine the operative ion transport mechanism, transport activity of **1d** was monitored in the presence of either carbonyl cyanide-4-(trifluoromethoxy) phenylhydrazone (FCCP, a proton transporter)^[23] or valinomycin (a K⁺ ion selective carrier).^[24] Under the applied pH gradient conditions ($\text{pH}_{\text{in}} = 7.0$ and $\text{pH}_{\text{out}} = 7.8$), **1d** (280 nM) displayed significantly enhanced transport activity in the presence of FCCP (937.5 nM) compared to that observed in the absence of FCCP (Figure S13). On the other hand, the transporting activity data of **1d** (340 nM) in the absence and presence of valinomycin (15 pM) were comparable (Figure S14). The FCCP and valinomycin coupled ion transport data corroborates to the OH⁻/Cl⁻ antiport as the main transport mechanism.^[25]

Subsequently, the Cl⁻ transport activity of **1d** and procarrier **2** across EYPC–LUVs⇌lucigenin were monitored at $\lambda_{\text{em}} = 535 \text{ nm}$ ($\lambda_{\text{ex}} = 455 \text{ nm}$) by applying a gradient of intravesicular NO₃⁻ and extravesicular Cl⁻.^[12] At comparable conditions, the compound **1d** showed significant Cl⁻ influx activity while compound **2** was inactive (Figure 2C). The concentration-dependent Cl⁻ influx study of **1d** across EYPC–LUVs⇌lucigenin provided $EC_{50} = 1.251 \mu\text{M}$ and $n = 2.047$ (Figure S16). The Hill

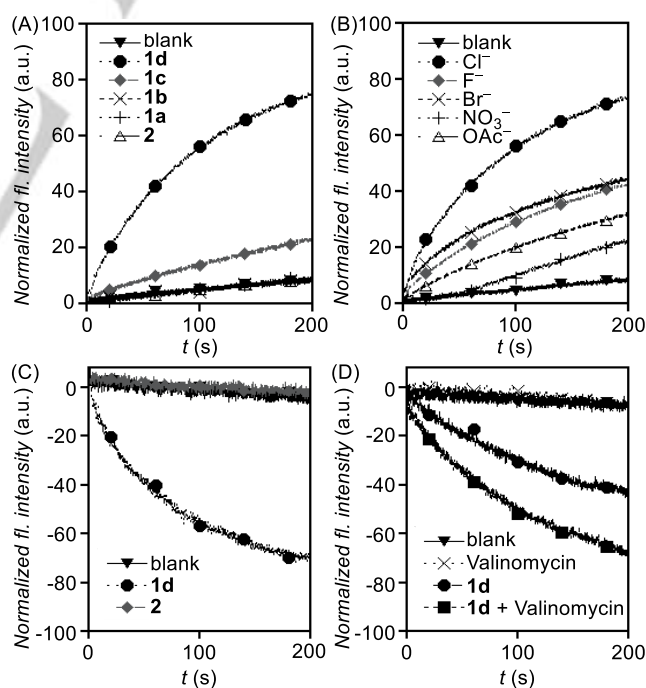


Figure 2. Comparison of ion transport activities of **1a-1d** and **2** (400 nM each) across EYPC–LUVs⇌HPTS (A). Anion selectivity of **1d** (340 nM) measured by varying the external anions of EYPC–LUVs⇌HPTS (B). Comparison of Cl⁻ influx activity of **1d** and **2** (2 μM each) across EYPC–LUVs⇌lucigenin (C). Comparison of Cl⁻ influx activity of **1d** (1.25 μM) in the absence and in the presence of valinomycin (1.25 μM) (D).

coefficient value further confirmed the involvement of two molecules of **1d** in the active transporter formation. The Cl⁻ influx activity of **1d** in the absence and presence of valinomycin were comparable, which further confirmed the antiport of anions as the main transport mechanism. (Figure 2D). The variation of extravesicular cation salts MCl (M = Li⁺, Na⁺, K⁺, Rb⁺, Cs⁺) did not show any change in transport activity further confirmed the anion antiport mechanism (Figure S17).

Based on the experimentally determined Hill coefficient value of ~ 2, the geometry-optimized structure of the [(**1d**)₂+Cl⁻] complex was obtained first by generating the most probable conformation by using CONFLEX 8 program (Figure S23),^[26] and subsequently optimizing the generated conformation by Gaussian 09 program^[27] using B3LYP functional and 6-311G(d,p) basis set.^[28] The geometry optimized structure of [(**1d**)₂+Cl⁻] complex indicated that two receptor molecules are orthogonally oriented around the central Cl⁻ ion (Figure S24A). The structure confirmed that each receptor participates in the anion recognition by N_{indole}-H_a...Cl⁻ (N_{indole}...Cl⁻ = 3.22 Å) as well as N_{amide}-H_b...Cl⁻ (N_{amide}...Cl⁻ = 3.38 Å) interactions (Figure S24B). In addition to these, the C_{ortho}...Cl⁻ distance = 3.75 Å and C_{ortho}-H_c...Cl⁻ bond angle ≈ 144.8° confirmed the presence of C_{ortho}-H_c...Cl⁻ interaction between a receptor and the ion.

The assessment of the photolytic conversion of procarrier **2** to the active transporter **1d** was confirmed by ¹H NMR. The solution of procarrier **2** in DMSO-*d*₆ (5 mg in 0.5 mL) was irradiated by 365 nm wavelength LED lamps with 5 min interval of time for 45 min. The H_a' signal of **2** at δ 11.78 disappeared upon photoirradiation with the appearance of a new signal at δ 11.81 that corresponds to the indole H_a, indicating the release of **1d** (Figure 3A). Similarly, the appearance of amide H_b signal at δ 10.52 ppm confirmed the cleavage of the ONB moiety from the indole-2-carboxamide. The disappearance of the H_c' signal at δ 5.45 ppm and the appearance of the new H_c signal at δ 11.66 ppm confirmed the formation of *o*-nitrosobenzaldehyde **8** as the photocleavage product.^[18c]

The successful release of the indole carboxamide **1d** upon photoirradiation of corresponding ONB protected derivative **2** prompted us studying the photoactivated membrane ion transport by **2**. For this purpose, the ion transport activities were monitored across EYPC-LUVs⊃HPTS under the pH gradient conditions (pH_{in} = 7.0 and pH_{out} = 7.8) after photoirradiating the samples of **2** (380 nM) for varied duration (i.e., irradiation time, *t*_R = 0, 1, 2, 3 and 5 min) in the presence of the LUVs (Figure S18A). During the ion transport experiments, the activities of these samples (i.e., relative fluorescence intensity) at 190 s after NaOH addition were compared by setting the HPTS fluorescence of blank sample to 0 and that of **1d** (380 nM) to 100. The nonirradiated sample of as-synthesized **2** was inactive (*F*_R = 1.7) as expected (Figure 3B). Upon irradiating **2** for *t*_R = 1min, the percent transport efficiency, *F*_R = 42.3 was recorded. It is interesting to note that up to 90.5% transport efficiency was achieved by irradiating the sample of **2** for just 3 min. A sample of 1% DMSO, when photoirradiated for 5 min under comparable conditions, gave only *F*_R = 0.1, which confirms that DMSO does not destroys the integrity of the lipid bilayer membrane.

Finally, the procarrier **2** and Cl⁻ carrier **1d** were evaluated for their cytotoxic effects in MCF 7 cell line. When the cells were incubated with the compound **2** for 24 h, no significant cytotoxicity was observed (Figure 3C). Surprisingly, compound **1d** also showed poor cytotoxicity. Interestingly, when the cells in the culture were analyzed under fluorescence microscope, significant precipitation of **1d** (10 μM) was observed in the extracellular media (Figure S22). Such precipitation was not observed for the compound **2**. Therefore, the poor cytotoxicity of **1d** was attributed to the low cell permeability of the compound.^[29] To check whether the procarrier can be subjected to photorelease within cells, the cells were incubated with compound **2** for 4 h and then irradiated with 365 nm light for 5 minutes. The cells were then kept in the incubator for 20 more h and monitored by standard MTT assay. The photoirradiated cells, incubated with compound **2**, showed pronounced cell death. However, photoirradiated control cells were completely viable (Figure 3C). The viability of the MCF 7 cells in the presence of *in situ* generated by-product (*o*-nitrosobenzaldehyde **8**) was evaluated independently and the compound showed negligible cytotoxicity compared to the photoreleased carrier **1d** (Figure S21). This data successfully established our proposition of inducing cell death by photoactivating Cl⁻ transport in cancer cells.

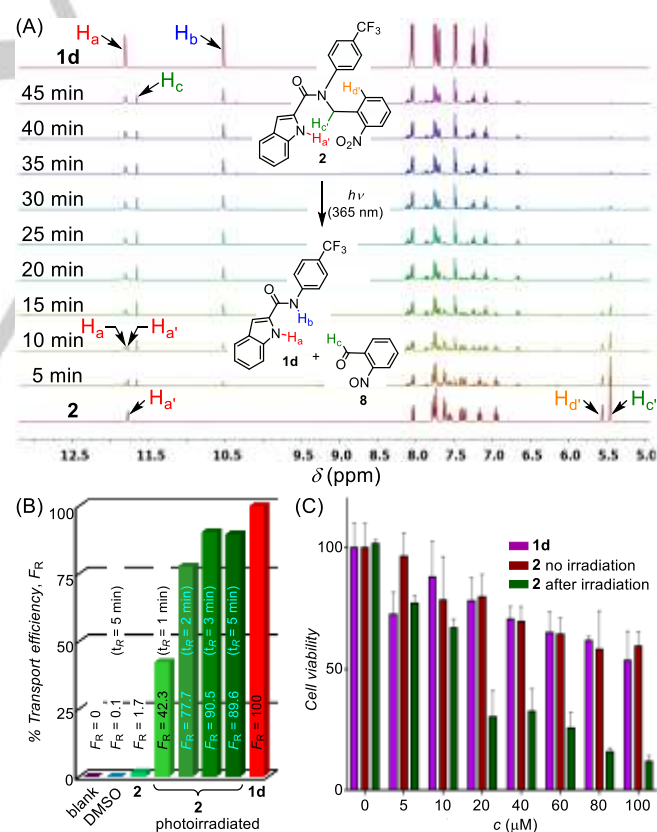


Figure 3. Phototriggered release of indole carboxamide **1d** from procarrier **2** monitored by ¹H NMR in DMSO-*d*₆ recorded at intervals of 5 min (A). Percent transport efficiencies of photoirradiated the samples measured relative to the activity of **1d** (B). Cell viability obtained from MTT assay upon addition **1d** and **2** for 24 h in MCF 7 cells. Mean cell viability was represented from three independent experiments (C).

In conclusion, we developed an *o*-nitrobenzyl (ONB) protected *N*-aryl-1*H*-indole-2-carboxamide procarrier that features efficient activation of membrane transport by cleaving its photolabile protecting group. The ONB protected procarrier with *p*-CF₃-phenyl as the aryl group was inactive while the free carboxamide was an efficient carrier of ion giving $EC_{50} = 0.219 \mu\text{M}$ and Hill coefficient, $n = 1.88$ when studied using EYPC-LUVs-HPTS. The carrier also exhibited Cl⁻/anion antiport across lipid bilayer membranes. The geometry optimized structure of the 2:1 carrier-Cl⁻ complex showed multivalent hydrogen bond interactions involved in the recognition of the anion. The mechanism of ONB photo-cleavage was also confirmed by the ¹H NMR study. The photocleavage of the ONB group facilitated up to 90.5% transport efficiency within 3 minutes of radiation. The photorelease of carrier **1d** from procarrier **2** within cancer cells and the resulting cell death were also confirmed by MTT assay. This rewarding outcome, based on our simple and innovative concept, can be extended in photodynamic therapy for surface cancer treatment and can also be adapted for deep-seated cancer therapy employing endoscopes or optical fibers.

Acknowledgements

This work was supported in part by collaborative grants from SERB, DST, Govt. of India (Grant No. EMR/2016/001897) and DBT (BT/HRD/NBA/36/06/2018). S.B.S. thanks DST, India for the Inspire Fellowship. We thank Sopan V. Shinde for valuable discussion.

Keywords: procarrier • photoactivation • anion binding • chloride selectivity • apoptosis

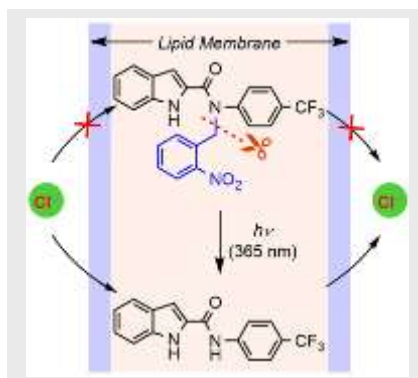
- [1] a) L. H. Pinto, G. R. Dieckmann, C. S. Gandhi, C. G. Papworth, J. Braman, M. A. Shaughnessy, J. D. Lear, R. A. Lamb, W. F. DeGrado, *Proc. Natl. Acad. Sci. U. S. A.* **1997**, *94*, 11301–11306; b) F. Lang, M. Föller, K. S. Lang, P. A. Lang, M. Ritter, E. Gulbins, A. Vereninov, S. M. Huber, *J. Membr. Biol.* **2005**, *205*, 147–157.
- [2] W. R. Sellers, D. E. Fisher, *J. Clin. Invest.* **1999**, *104*, 1655–1661.
- [3] a) J. M. Brown, L. D. Attardi, *Nat. Rev. Cancer* **2005**, *5*, 231–237; b) L. Portt, G. Norman, C. Clapp, M. Greenwood, M. T. Greenwood, *Biochim. Biophys. Acta* **2011**, *1813*, 238–259.
- [4] R. S. Y. Wong, *J. Exp. Clin. Cancer Res.* **2011**, *30*, 87.
- [5] F. H. Igney, P. H. Krammer, *Nat. Rev. Cancer* **2002**, *2*, 277–288.
- [6] a) S. Matile, A. Vargas Jentsch, J. Montenegro, A. Fin, *Chem. Soc. Rev.* **2011**, *40*, 2453–2474; b) T. M. Fyles, *Chem. Soc. Rev.* **2007**, *36*, 335–347; c) P. V. Santacrose, J. T. Davis, M. E. Light, P. A. Gale, J. C. Iglesias-Sánchez, P. Prados, R. Quesada, *J. Am. Chem. Soc.* **2007**, *129*, 1886–1887; d) O. A. Okunola, J. L. Seganish, K. J. Salimian, P. Y. Zavalij, J. T. Davis, *Tetrahedron* **2007**, *63*, 10743–10750.
- [7] R. Pérez-Tomás, B. Montaner, E. Llagostera, V. Soto-Cerrato, *Biochem. Pharmacol.* **2003**, *66*, 1447–1452.
- [8] P. Manuel-Manresa, L. Korrodi-Gregório, E. Hernando, A. Villanueva, D. Martínez-García, A. M. Rodilla, R. Ramos, M. Fardilha, J. Moya, R. Quesada, V. Soto-Cerrato, R. Perez-Tomas, *Mol. Cancer Ther.* **2017**, *16*, 1224–1235.
- [9] a) N. Busschaert, M. Wenzel, M. E. Light, P. Iglesias-Hernández, R. Pérez-Tomás, P. A. Gale, *J. Am. Chem. Soc.* **2011**, *133*, 14136–14148; b) S. J. Moore, C. J. E. Haynes, J. González, J. L. Sutton, S. J. Brooks, M. E. Light, J. Herniman, G. J. Langley, V. Soto-Cerrato, R. Pérez-Tomás, I. Marques, P. J. Costa, V. Félix, P. A. Gale, *Chem. Sci.* **2013**, *4*, 103–117.
- [10] S.-K. Ko, S. K. Kim, A. Share, V. M. Lynch, J. Park, W. Namkung, W. Van Rossom, N. Busschaert, P. A. Gale, J. L. Sessler, I. Shin, *Nat. Chem.* **2014**, *6*, 885–892.
- [11] N. Busschaert, S.-H. Park, K.-H. Baek, Y. P. Choi, J. Park, E. N. W. Howe, J. R. Hiscock, L. E. Karagiannidis, I. Marques, V. Félix, W. Namkung, J. L. Sessler, P. A. Gale, I. Shin, *Nat. Chem.* **2017**, *9*, 667–675.
- [12] T. Saha, M. S. Hossain, D. Saha, M. Lahiri, P. Talukdar, *J. Am. Chem. Soc.* **2016**, *138*, 7558–7567.
- [13] a) E. N. W. Howe, N. Busschaert, X. Wu, S. N. Berry, J. Ho, M. E. Light, D. D. Czech, H. A. Klein, J. A. Kitchen, P. A. Gale, *J. Am. Chem. Soc.* **2016**, *138*, 8301–8308; b) N. Busschaert, R. B. P. Elmes, D. D. Czech, X. Wu, I. L. Kirby, E. M. Peck, K. D. Hendzel, S. K. Shaw, B. Chan, B. D. Smith, K. A. Jolliffe, P. A. Gale, *Chem. Comm.* **2014**, *5*, 3617–3626; c) A. Roy, O. Biswas, P. Talukdar, *Chem. Comm.* **2017**, *53*, 3122–3125; d) S. V. Shinde, P. Talukdar, *Angew. Chem. Int. Ed.* **2017**, *56*, 4238–4242.
- [14] a) Y. R. Choi, B. Lee, J. Park, W. Namkung, K.-S. Jeong, *J. Am. Chem. Soc.* **2016**, *138*, 15319–15322; b) E. B. Park, K.-S. Jeong, *Chem. Comm.* **2015**, *51*, 9197–9200.
- [15] Y. R. Choi, G. C. Kim, H.-G. Jeon, J. Park, W. Namkung, K.-S. Jeong, *Chem. Comm.* **2014**, *50*, 15305–15308.
- [16] a) J. A. Barltrop, P. Schofield, *Tetrahedron Lett.* **1962**, *3*, 697–699; b) J. A. Barltrop, P. J. Plant, P. Schofield, *Chem. Comm.* **1966**, 822–823.
- [17] a) A. P. Pelliccioli, J. Wirz, *Photochem. Photobiol. Sci.* **2002**, *1*, 441–458; b) P. Klán, T. Šolomek, C. G. Bochet, A. Blanc, R. Givens, M. Rubina, V. Popik, A. Kostikov, J. Wirz, *Chem. Rev.* **2013**, *113*, 119–191.
- [18] a) I. R. Dunkin, J. Gębicki, M. Kiszka, D. Sanín-Leira, *J. Chem. Soc., Perkin Trans. 2* **2001**, 1414–1425; b) X. Bai, Z. Li, S. Jockusch, N. J. Turro, J. Ju, *Proc. Natl. Acad. Sci. U. S. A.* **2003**, *100*, 409–413; c) Y. V. Il'ichev, M. A. Schwörer, J. Wirz, *J. Am. Chem. Soc.* **2004**, *126*, 4581–4595.
- [19] a) N.-C. Fan, F.-Y. Cheng, J.-a. A. Ho, C.-S. Yeh, *Angew. Chem., Int. Ed.* **2012**, *51*, 8806–8810; b) J. Liu, W. Bu, L. Pan, J. Shi, *Angew. Chem., Int. Ed.* **2013**, *52*, 4375–4379; c) W. S. Shin, J. Han, R. Kumar, G. G. Lee, J. L. Sessler, J.-H. Kim, J. S. Kim, *Sci. Rep.* **2016**, *6*, 29018; d) Y. Yang, J. Mu, B. Xing, *Wiley Interdiscip. Rev. Nanomed. Nanobiotechnol.* **2017**, *9*, e1408.
- [20] a) R. Reinhard, B. F. Schmidt, *J. Org. Chem.* **1998**, *63*, 2434–2441; b) W. Lin, D. Peng, B. Wang, L. Long, C. Guo, J. Yuan, *Eur. J. Org. Chem.* **2008**, *2008*, 793–796; c) S. K. Choi, M. Verma, J. Silpe, R. E. Moody, K. Tang, J. J. Hanson, J. R. Baker, *Bioorganic Med. Chem.* **2012**, *20*, 1281–1290; d) S. Mo, Y. Wen, F. Xue, H. Lan, Y. Mao, G. Lv, T. Yi, *Sci. Bull.* **2016**, *61*, 459–467.
- [21] Marvin 5.8.0, ChemAxon, 2012 (<http://www.chemaxon.com>)
- [22] a) BindFit v0.5. <http://app.supramolecular.org/bindfit/> (accessed July 2017); b) P. Thordarson, *Chem. Soc. Rev.* **2011**, *40*, 1305–1323.
- [23] R. Benz, S. McLaughlin, *Biophys. J.* **1983**, *41*, 381–398.
- [24] L. Rose, A. T. A. Jenkins, *Bioelectrochemistry* **2007**, *70*, 387–393.
- [25] T. Saha, S. Dasari, D. Tewari, A. Prathap, K. M. Sureshan, A. K. Bera, A. Mukherjee, P. Talukdar, *J. Am. Chem. Soc.* **2014**, *136*, 14128–14135.
- [26] a) H. Goto, S. Obata, N. Nakayama, K. Ohta, CONFLEX 8, CONFLEX Corporation, Tokyo, Japan, 2012; b) H. Goto, E. Osawa, *J. Am. Chem. Soc.* **1989**, *111*, 8950–8951.
- [27] M. J. Frisch, et al., *Gaussian 09*, Revision B.01; Gaussian, Inc.: Wallingford, CT, 2010.
- [28] A. D. McLean, G. S. Chandler, *J. Chem. Phys.* **1980**, *72*, 5639–5648.
- [29] a) D. Jornada, G. dos Santos Fernandes, D. Chiba, T. de Melo, J. dos Santos, M. Chung, *Molecules* **2016**, *21*, 42; b) S. V. Gupta, D. Gupta, J. Sun, A. Dahan, Y. Tsume, J. Hilfinger, K.-D. Lee, G. L. Amidon, *Mol. Pharm.* **2011**, *8*, 2358–2367.

Entry for the Table of Contents

Layout 1:

COMMUNICATION

A photocleavable procarrier is reported to release a transmembrane chloride carrier. Such photorelease of the active carrier in cancer cells resulted in a remarkable cell death.



Swati Bansi Salunke, Javid Ahmad Malla, Dr. Pinaki Talukdar*

Page No. – Page No.

Phototriggered release of transmembrane chloride carrier from an o-nitrobenzyl-linked procarrier